EURASIP Journal on Applied Signal Processing 2005:10, 1554–1565

Time-Frequency (Wigner) Analysis of Linear and Nonlinear Pulse Propagation in Optical Fibers

José Azaña

Institut National de la Recherche Scientifique, Énergie, Matériaux et Télécommunications, 800 de la Gauchetière Ouest, bureau 6900, Montréal, QC, Canada H5A 1K6
Email: azana@emt.inrs.ca

Received 12 April 2004; Revised 7 June 2004

Time-frequency analysis, and, in particular, Wigner analysis, is applied to the study of picosecond pulse propagation through optical fibers in both the linear and nonlinear regimes. The effects of first- and second-order group velocity dispersion (GVD) and self-phase modulation (SPM) are first analyzed separately. The phenomena resulting from the interplay between GVD and SPM in fibers (e.g., soliton formation or optical wave breaking) are also investigated in detail. Wigner analysis is demonstrated to be an extremely powerful tool for investigating pulse propagation dynamics in nonlinear dispersive systems (e.g., optical fibers), providing a clearer and deeper insight into the physical phenomena that determine the behavior of these systems.

Keywords and phrases: Wigner distributions, dispersive media, nonlinear fiber optics, optical pulse propagation and solitons.

1. INTRODUCTION

The study of optical pulse propagation in optical fibers is interesting from both fundamental and applied perspectives. Understanding the physics behind the processes that determine the evolution of optical pulses in single-mode fibers is essential for the design and performance analysis of optical fiber communication systems. As an example, it is well known that in intensity-modulated direct-detection (IM/DD) systems, the combined effects of source chirping, group velocity dispersion (GVD) and, for long-haul or high-power systems, self-phase modulation (SPM) cause distortion of the propagating signals [1]. This distortion essentially limits the maximum achievable bit rates and transmission distances. The influence of fiber GVD and fiber nonlinearities (e.g., SPM) on the performance of communication systems is becoming more critical in view of the expected evolution of fiber optics communications systems [2], in particular, (i) the channel data rates are expected to continue increasing, with 40 and 80 Gbps rate systems now under development; and (ii) the communication strategies (e.g., dense-wavelength-division-multiplexing, DWDM, strategies) tend to increase the number of channels and information (i.e., the signal power) launched into a single fiber.

For the study of the dynamics of pulse propagation in fibers, the involved signals (optical pulses) can be represented in either the temporal or the frequency domains. However, since these signals are intrinsically nonstationary (i.e., the spectrum content changes as a function of time), these conventional one-dimensional representations provide only partial information about the analyzed signals and, consequently, about the system under study. In this paper, we analyze linear and nonlinear pulse propagation in optical fibers using joint time-frequency (TF) representations [3]. Our analysis is based on the representation of the events of interest (optical pulses propagating through the fiber) in the joint TF plane, that is, the signals are represented as two-dimensional functions of the two variables time and frequency, simultaneously. For the TF representation, we will use the well-known Wigner distribution function. The Wigner distribution exhibits a lot of mathematical properties that make this approach especially attractive for the problem under consideration. For instance, as compared with other well-known methods for the TF representation of optical pulses (e.g., spectrograms [3]), the Wigner distribution provides an improved joint TF resolution. Note that this is a critical aspect for extracting detailed information about the events under analysis from the resultant images. The discussion of other attractive properties of the Wigner distribution is out of the scope of this work but the interested reader can find a good review article on the fundaments and applications of Wigner analysis by Dragoman in this same special issue or can refer to other classical papers in the subject [4].

TF representations in general, and Wigner analysis in particular, have been used in the past for the analysis of (ultra-) short light pulses and, in particular, these methods have been applied to investigating (i) simple linear optical systems (e.g., Fabry-Perot filters, fiber Bragg gratings) [5, 6], (ii) soliton waveforms [5, 7], and (iii) optical pulse-compression operations [8]. TF techniques have been

also evaluated as alternative methods for measuring optical fiber dispersion (linear regime) [9]. More recently, TF representations (spectrograms) have been applied to the analysis of specific phenomena (e.g., continuum generation) in *nonlinear* optical fiber devices [10, 11] but these recent works deal with optical pulses in the femtosecond range, a regime which is of less interest in the context of fiber optics communications (optical pulses in the picosecond range).

In this paper, the Wigner distribution is applied to the study of the *dynamics* of linear and nonlinear *picosecond* pulse propagation in optical fibers. By means of a few examples, we demonstrate that the Wigner analysis offers a simple and easy-to-interpret representation of the linear and nonlinear dynamics in fibers within the picosecond regime, providing in fact a profound insight into the physics behind the phenomena that determine the optical pulse evolution through the fibers. The information provided by the Wigner technique complements that given by other analysis methods and offers a clearer and deeper understanding of the phenomena under study. It should be also mentioned that the discussion in this present work is restricted to the case of completely coherent light distributions. The Wigner formalism has been previously applied to the analysis of propagation of partially coherent light through nonlinear media, leading in fact to the description of phenomena not discussed here [12].

The remainder of this paper is structured as follows. In Section 2, the theoretical fundaments of our analysis are established. In particular, the nonlinear Schrödinger equation (NLSE) for modeling picosecond pulse propagation in optical fibers is briefly reviewed and the Wigner distribution function used throughout the work is defined as well. In Section 3, we conduct Wigner analysis of picosecond optical pulse propagation through optical fibers operating in the linear regime. The impact of first- and second-order dispersions are analyzed in detail. Section 4 is devoted to the Wigner analysis of picosecond optical pulse propagation through nonlinear optical fibers. The interplay of GVD and SPM is analyzed in both the normal and anomalous dispersion regimes. Finally, in Section 5, we conclude and summarize.

2. THEORETICAL FUNDAMENTS

The propagation of optical pulses in the picosecond range through a lossless single-mode optical fiber can be described by the well-known NLSE [1]:

$$i\frac{\partial A(z,\tau)}{\partial z} - \frac{\beta_2}{2}\frac{\partial^2 A(z,\tau)}{\partial \tau^2} + \gamma\left|A(z,\tau)\right|^2 A(z,\tau) = 0, \quad (1)$$

where $A(z,\tau)$ is the complex envelope of the optical pulse (pulse centered at the frequency ω_0), z is the fiber length, and τ represents the time variable in the so-called retarded frame (i.e., temporal frame with respect to the pulse group delay), $\beta_2 = [\partial^2\beta(\omega)/\partial\omega^2]_{\omega=\omega_0}$ is the first-order GVD ($\beta(\omega)$ is the propagation constant of the single-mode fiber), and γ is the nonlinear coefficient of the fiber. In most cases, (1) and its modifications cannot be solved analytically and one has to use numerical approaches. Here we will use the most commonly applied numerical scheme for solving the NLSE, the so-called split-step Fourier transform (SSFT) method [13].

In order to characterize the fiber distances over which dispersive and nonlinear effects are important, two parameters are usually used, namely, the dispersion length L_D and the nonlinear length L_{NL}, [1]

$$L_D = \frac{T_0^2}{|\beta_2|}, \qquad L_{NL} = \frac{1}{\gamma P_0}, \quad (2)$$

where T_0 and P_0 are the time width and peak power of the pulse launched at the input of the fiber $A(0,\tau)$. Depending on the relative magnitudes of L_D, L_{NL}, and the fiber length z, the propagation behavior is mainly determined by dispersive effects, by nonlinear effects or by interplay between both dispersive and nonlinear effects (when both contributions are significant).

Once the NLSE in (1) is solved for the specific problem under study, our subsequent study will be based on the detailed analysis of the obtained pulse complex envelope $A(z,\tau)$. For a given fiber length ($z \equiv$ constant), this signal can be represented either in the temporal domain (as directly obtained from (1)) or in the spectral domain,

$$\tilde{A}(z,\omega) = \Im[A(z,\tau)] = \left(\frac{1}{\sqrt{2\pi}}\right)\int_{-\infty}^{+\infty} A(z,\tau)\exp(-j\omega\tau)d\tau, \quad (3)$$

where $\Im$ is the Fourier transform operator. A more profound insight into the nature of the pulse under analysis can be obtained if this pulse is represented in the joint time-frequency phase space. For this purpose, we will use the time-resolved Wigner distribution function, $W_z(\tau,\omega)$, which will be calculated as follows [3]:

$$W_z(\tau,\omega) = \int_{-\infty}^{+\infty} A\left(z,\tau+\frac{\tau'}{2}\right)A^*\left(z,\tau-\frac{\tau'}{2}\right)\exp[-i\omega\tau']d\tau'. \quad (4)$$

The Wigner distribution allows us to represent the signal propagating through the fiber $A(z,\tau)$ in the two domains, time and frequency, simultaneously, that is, the signal is mapped into a 2D image which essentially represents the signal's joint time-frequency energy distribution. This 2D image displays the link between the temporal and spectral pulse features in a very simple and direct way, thus providing broader information on the signal and system under analysis.

3. WIGNER ANALYSIS OF LINEAR PULSE PROPAGATION IN OPTICAL FIBERS

When the fiber length z is such that $z \ll L_{NL}$ and $z \ll L_D$, then neither dispersive nor nonlinear effects play a significant role during pulse propagation and as a result, the pulse

maintains its shape during propagation $A(z,\tau) = A(0,\tau)$. This case is obviously out of the interest of this work. When the fiber length is such that $z \ll L_{NL}$ but $z \approx L_D$, then the pulse evolution is governed by GVD and the nonlinear effects play a relatively minor role. More specifically, the dispersion-dominant regime is applicable when the following condition is satisfied:

$$\frac{L_D}{L_{NL}} = \frac{\gamma P_0 T_0^2}{|\beta_2|} \ll 1. \tag{5}$$

In this case, the last term in the left-hand side of the NLSE in (1) (i.e., the nonlinear term) can be neglected and the optical fiber can be modeled as a linear time-invariant system (i.e., as a filter). Specifically, the fiber operates as a phase-only filter which only affects the phase of the spectral content of the signal propagating through it. This phase-only filtering process is in fact determined by the GVD characteristic of the optical fiber and, in particular,

$$\tilde{A}(z,\omega) \propto \tilde{A}(0,\omega) \exp\left(-i\frac{\beta_2}{2} z\omega^2\right), \tag{6}$$

where the symbol $\propto$ indicates that the two terms are proportional.

The propagation regime where nonlinearities can be neglected is typical of optical communication systems when the launched signals exhibit a relatively low power. As a rough estimate, in order to ensure operation within the linear regime, the peak power of the input pulses must be $P_0 \ll 1\,\mathrm{W}$ for 1-picosecond pulses in conventional single-mode fiber operating at the typical telecommunication wavelength of $\lambda \approx 1.55\,\mu\mathrm{m}$ ($\omega_0 \approx 2\pi \times 193.4\,\mathrm{THz}$).

3.1. First-order dispersion of a transform-limited optical pulse

In the first example (results shown in Figure 1), the propagation of an optical pulse through a first-order dispersive fiber in the linear regime is analyzed. In particular, we assume a fiber with a first-order dispersion coefficient $\beta_2 = -20\,\mathrm{ps^2Km^{-1}}$ (typical value in a conventional single-mode fiber working at $\lambda \approx 1.55\,\mu\mathrm{m}$). This regime is usually referred to as anomalous dispersion regime ($\beta_2 < 0$). Figure 1 shows the Wigner representation of the optical pulse envelope $A(z,\tau)$ evaluated at different fiber propagation distances, $z = 0$ (input pulse), $z = 0.5\,L_D$, $z = 2\,L_D$, and $z = 6\,L_D$ ($L_D \approx 450\,\mathrm{m}$). For each representation, the plot at the left shows the spectral energy density of the optical pulse $|\tilde{A}(z,\omega)|^2$, the plot at the bottom shows the average optical intensity of the pulse $|A(z,\tau)|^2$, and the larger plot in the upper right of the representations shows the Wigner distribution of the pulse $W_z(\tau,\omega)$. Note that this distribution is plotted as a 2D image where the relative brightness levels of the image represent the distribution intensity and, in particular, darker regions in the image correspond to higher intensities. This 2D image provides information about the temporal location of the signal spectral components or in other words, it shows which of the spectral components of the signal occur at each instant of time.

The input pulse is assumed to be a transform-limited super-Gaussian pulse, $A(0,\tau) = \sqrt{P_0}\exp[(-1/2)(\tau/T_0)^{2m}]$, where $m = 3$, $T_0 = 3$ picoseconds and the peak power P_0 is low enough to ensure operation within the linear regime (i.e., to ensure that the fiber nonlinearities are negligible). In this paper, super-Gaussian pulses will be used as input signals because they are more suited than for instance Gaussian pulses to illustrate the effects of steep leading and trailing edges while providing similar information on the physics behind the different linear and nonlinear phenomena to be investigated. The Wigner distribution of this input pulse is typical of a transform-limited signal where all the spectral components exhibit the same mean temporal delay. Since the fiber operates as a phase-only filter, the energy spectrum of the pulse is not affected by the propagation along the optical fiber. In other words, the optical pulse propagating through the fiber retains identical spectral components to those of the incident pulse. However, due to the GVD introduced by the fiber, these spectral components are temporally realigned according to the group delay curve of the fiber. This temporal realignment of the pulse spectral components is responsible for the distortion and broadening of the temporal shape of the pulse as it propagates along the fiber and can be easily understood and visualized through the Wigner representations shown in Figure 1. The dispersion-induced pulse temporal broadening is a detrimental phenomenon for optical communication purposes. As a result of this temporal broadening, the adjacent pulses in a sequence launched at the input of the fiber (this pulse sequence can carry coded information to be transmitted through the fiber) can interfere with each other and this interference process can obviously limit the proper recovering of the information coded in the original sequence [2].

We remind the reader that the group delay in a first-order dispersive fiber is a linear function of frequency and depends linearly on the fiber distance z as well. This is in good agreement with the temporal realignment process that can be inferred from the Wigner distributions shown in Figure 1. More specifically, the pulse spectral components separate temporally from each other as they propagate through the fiber. In fact, as the Wigner representation of the pulse at $z = 6\,L_D$ shows, for a sufficiently long fiber distance, the temporal realignment process of the pulse spectral components is sufficiently strong so that only a single dominant frequency term exists at each given instant of time. This can be very clearly visualized in the corresponding Wigner representation: the signal distributes its energy along a straight line in the TF plane. In this case, there is a direct correspondence between time and frequency domains or in other words, the temporal and spectral pulse shapes are proportional, $|A(z,\tau)| \propto |\tilde{A}(z,\omega)|_{\omega=\tau/\beta_2 z}$. This frequency-to-time conversion operation induced by simple propagation of an optical pulse through a first-order dispersive medium (e.g., an optical fiber) is usually referred to as *real-time Fourier*

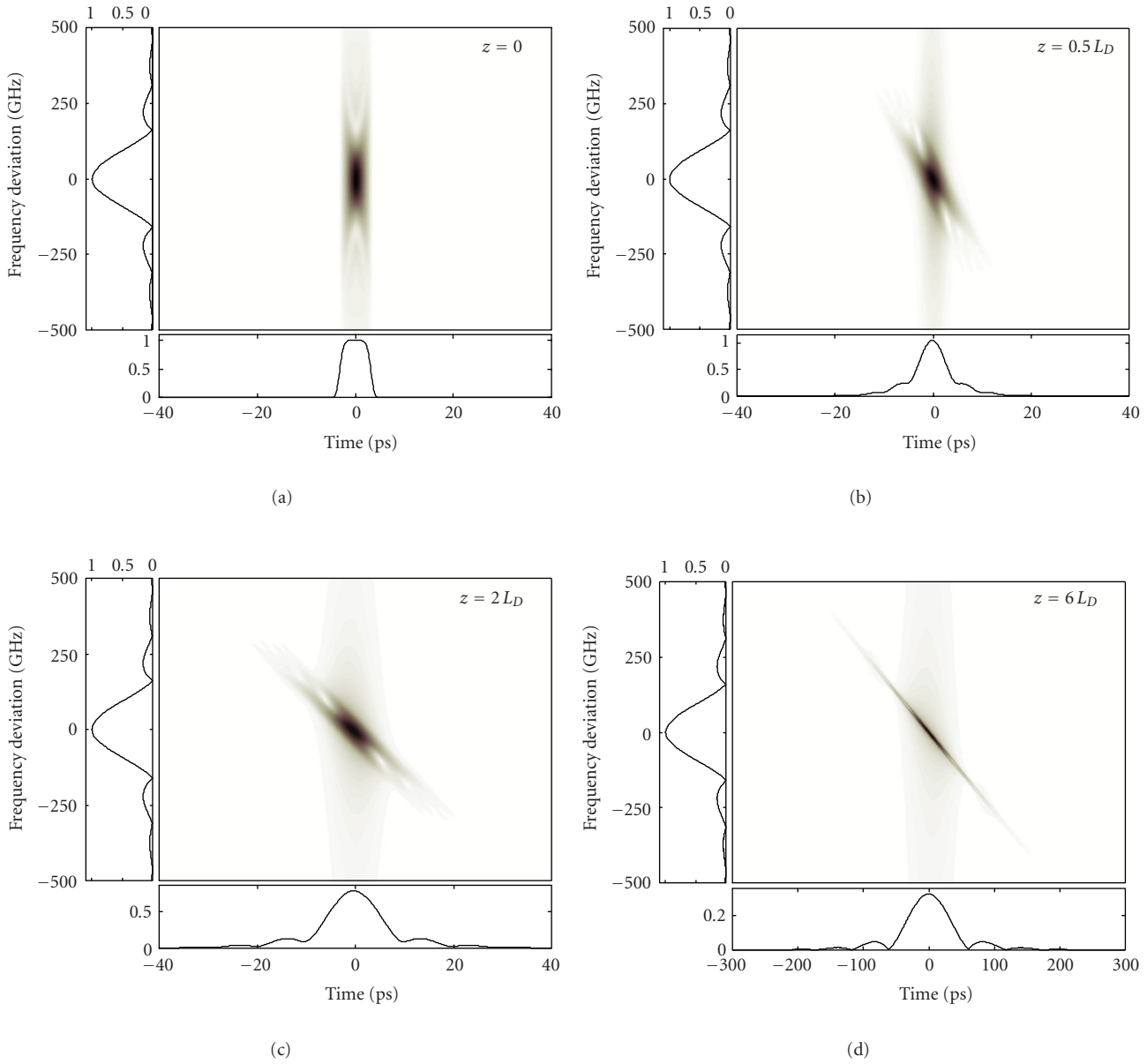

Figure 1: Wigner analysis of linear pulse propagation in an optical fiber (first-order dispersion).

transformation (RTFT) [14]. The exact condition to ensure RTFT of the input optical pulse is the following [15]:

$$z \gg \frac{T^2}{8\pi\,|\beta_2|}. \tag{7}$$

RTFT has been demonstrated for different interesting applications, including real-time optical spectrum analysis, fiber dispersion measurements [14], and temporal and spectral optical pulse shaping [15, 16]. An interesting application of the phenomenon for monitoring channel crosstalk in DWDM optical communication networks is also described in detail in the paper by Llorente et al. in this present special issue.

3.2. First-order dispersion of a chirped optical pulse

In the second example (results shown in Figure 2), the propagation of a nontransform-limited optical pulse through the same optical fiber as in the previous example is analyzed. In this case, we assume a chirped super-Gaussian input pulse $A(0,\tau) = \sqrt{P_0}\exp[(-[1+iC]/2)(\tau/T_0)^{2m}]$, where $m = 3, T_0 = 3$ picoseconds, and the peak power P_0 is again assumed to be low enough to ensure operation within the linear regime. The new parameter C is referred to as the chirp of the pulse and is used to model a phase variation across the temporal profile of the pulse. In our example, we fix $C = -3$. Pulses generated from semiconductor or mode-locked laser are typically chirped and that is why it is important also to evaluate the effect of pulse chirp on the dispersion process.

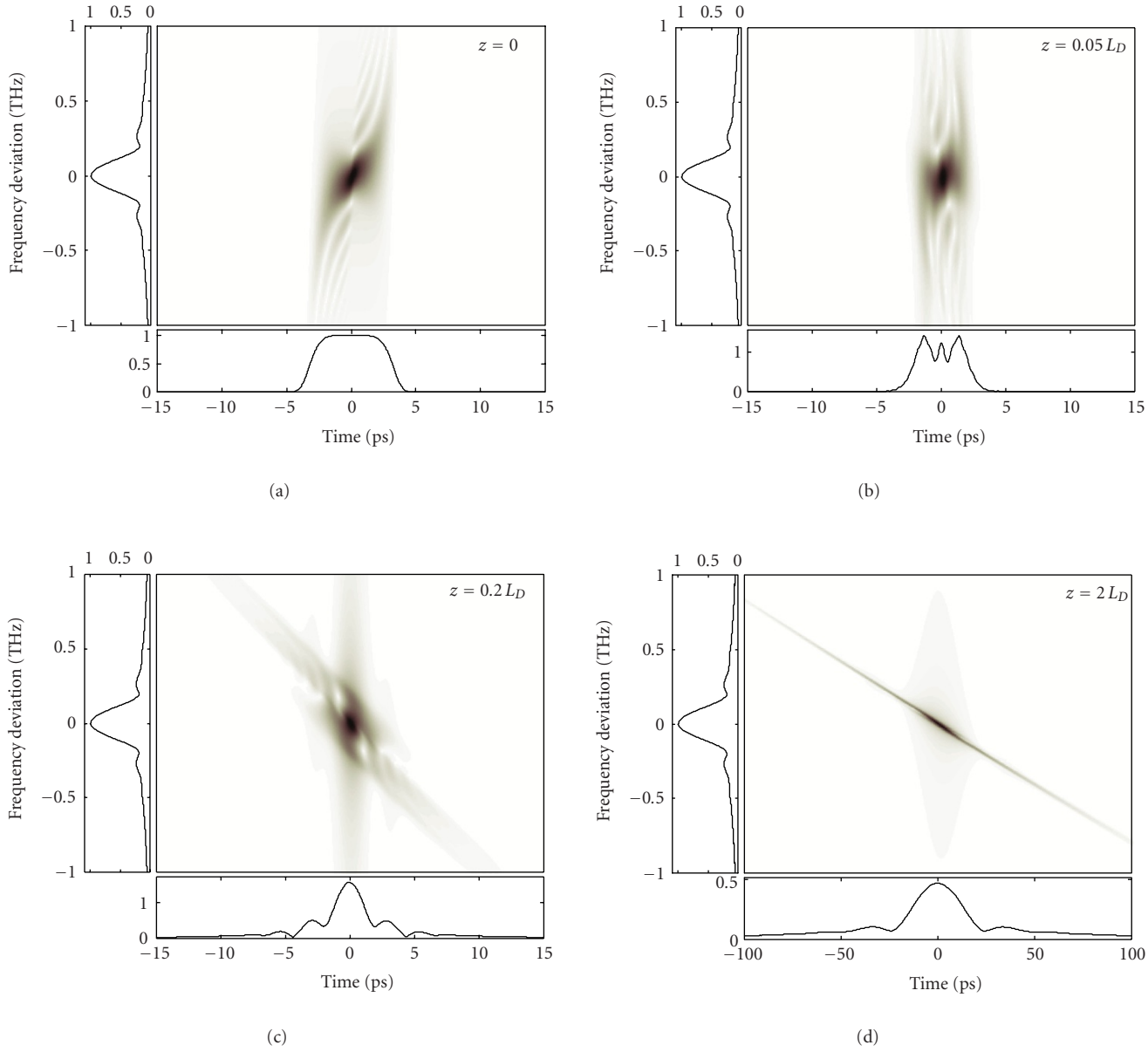

Figure 2: Wigner analysis of linear propagation of a chirped optical pulse through an optical fiber (first-order dispersion).

Figure 1 analyzes the optical pulse envelope $A(z, \tau)$ evaluated at different fiber propagation distances, $z = 0$ (input pulse), $z = 0.05\,L_D$, $z = 0.2\,L_D$, and $z = 2\,L_D$. As shown in the plot corresponding to the input pulse ($z = 0$), the temporal shape (amplitude) of this pulse is identical to that of the corresponding unchirped (transform-limited) pulse (example shown in Figure 1) but the energy spectrum differs significantly from that of the unchirped case. Similarly, the Wigner distribution clearly corresponds with a nontransform-limited pulse as the different pulse spectral components exhibit now a different mean time delay. In particular, the frequencies in the low-frequency and high-frequency sidelobes lie in the leading and trailing edges of the temporal pulse, respectively, whereas the frequencies in the main spectral lobe are associated with the central, high-energy part of the temporal pulse. The effect of propagation of the chirped pulse through the initial section of the first-order dispersive fiber is essentially different to that observed for the case of a transform-limited pulse. The effect of the fiber medium on the optical pulse can be again modeled as a phase-only filtering process as that described by (6). However, in the initial section of the fiber, the GVD introduced by the fiber will compensate partially the intrinsic positive chirp of the original pulse so that the pulse will undergo temporal compression (instead of temporal broadening as it is typical of transform-limited pulses). For a specific

fiber length, the pulse will undergo its maximum temporal compression (approximately for $z = 0.05\,L_D$, in the example shown here) when total chirp compensation is practically achieved. The Wigner distribution of the pulse confirms that in the case of maximum compression this pulse is approximately a transform-limited signal (where all the spectral components have the same mean time delay). Ideal chirp compensation with a first-order dispersive medium can be only achieved if the original pulse exhibits an ideal linear chirp (in our case, the input pulse exhibits a quadratic chirp). The described compression process of chirped optical pulses using propagation through a suitable dispersive medium has been extensively applied for pulse-compression operations aimed to the generation of (ultra-) short optical pulses [17]. In fact, optical pulse-compression operations have been analyzed in the past using Wigner representations [8]. As the plots corresponding to $z = 0.2\,L_D$ and $z = 2\,L_D$ show, further propagation in the optical fiber after the optimal compression length has a similar effect to that described for the case of transform-limited pulses. Briefly, the spectral components of the pulse are temporally separated thus causing the consequent distortion and broadening of the temporal pulse shape. For sufficiently long fiber distance, a frequency-to-time conversion process (RTFT) can be also achieved (e.g., $z = 2\,L_D$).

3.3. Second-order dispersion of a transform-limited optical pulse

The contribution of second-order dispersion on optical pulses can be introduced in the previous NLSE equation by including the corresponding term as follows:

$$i\frac{\partial A(z,\tau)}{\partial z} - \frac{\beta_2}{2}\frac{\partial^2 A(z,\tau)}{\partial \tau^2} + i\frac{\beta_3}{6}\frac{\partial^3 A(z,\tau)}{\partial \tau^3} + \gamma\left|A(z,\tau)\right|^2 A(z,\tau) = 0, \tag{8}$$

where $\beta_3 = [\partial^3\beta(\omega)/\partial\omega^3]_{\omega=\omega_0}$ is the second-order GVD. The contribution of the second-order dispersion induced by the fiber medium on optical pulses in the picosecond range can be normally neglected as compared with the contribution of the first-order dispersion factor. For optical pulses in the picosecond range, this second-order dispersion contribution becomes important only when the fibers are operated in the vicinity of the so-called zero-dispersion wavelength, where the first-order dispersion coefficient is null. Operating around the fiber zero-dispersion wavelength can be of interest for applications where fiber dispersion must be minimized, for example, to exploit some nonlinearities in the fiber [9]. Conventional single-mode fiber (such most of the fiber currently deployed for optical communication purposes) exhibits zero dispersion around 1.3 μm (the dispersion problem described above is still present at 1.55 μm in this kind of fibers) but especial fiber designs allow shifting the zero-dispersion wavelength to the desired value (e.g., 1.55 μm).

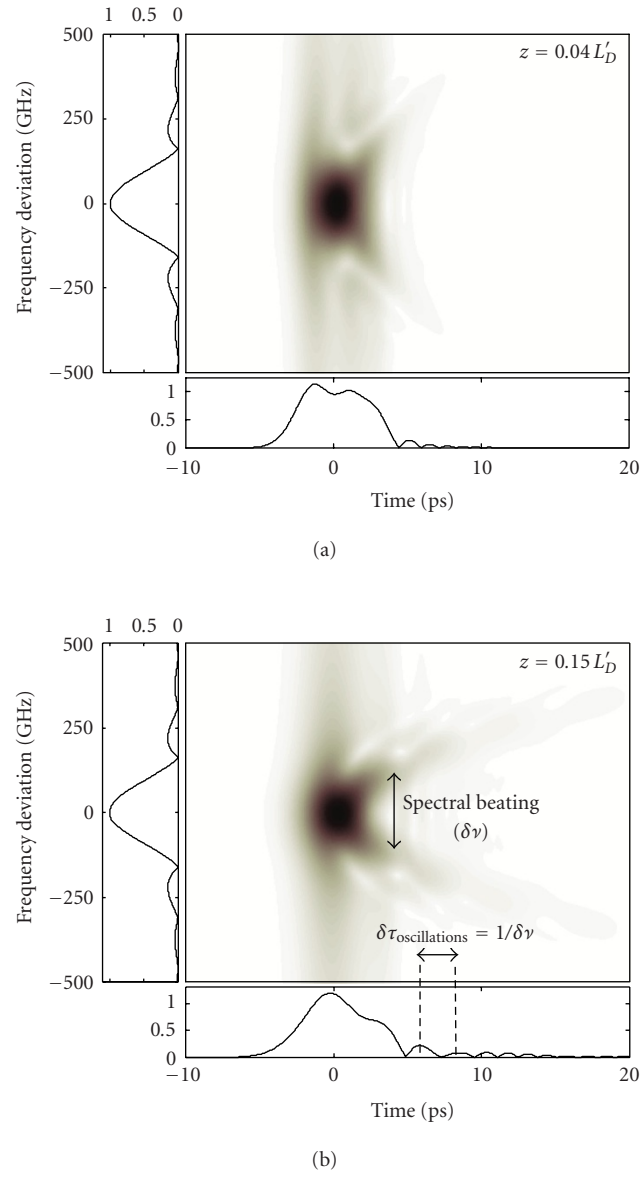

Figure 3: Wigner analysis of linear pulse propagation in an optical fiber (second-order dispersion).

If the first-order dispersion coefficient is null, then the effect of second-order dispersion must be taken into account. In order to evaluate the impact of second-order dispersion on an optical pulse, we will assume that the fiber nonlinearities are negligible as well. In this case, the second and fourth term in the left-hand side of (8) can be neglected and as a result, the optical fiber operates as a linear time-invariant system (i.e., as a filter). In particular,

$$\tilde{A}(z,\omega) \propto \tilde{A}(0,\omega)\exp\left(-j\frac{\beta_3}{2}z\omega^3\right). \tag{9}$$

In Figure 3, the propagation of a super-Gaussian optical pulse similar to that shown in Figure 1 ($z = 0$) through a

second-order dispersive fiber with $\beta_3 = -0.1\,\text{ps}^3\text{Km}^{-1}$ (typical value in a conventional single-mode fiber working at $\lambda \approx 1.3\,\mu$m) is analyzed. In particular, the pulse envelope is analyzed at the fiber distances $z = 0.04\,L_D'$ and $z = 0.15\,L_D'$ where $L_D' = T_0^3/|\beta_3| \approx 270\,\text{Km}$. As expected, the original pulse spectrum is not affected during propagation through the fiber. The Wigner distributions show that these spectral components undergo however a temporal realignment according to the GVD characteristic of the device which in turn causes the observed distortion in the temporal pulse shape. This temporal realignment of the pulse spectral components is very different from that observed in the case of first-order dispersion (compare with Figure 1) as the GVD characteristics in both fibers are different. In the case of second-order dispersion, the original pulse evolves towards a nonsymmetric temporal shape which consists of two components, a main high-energy pulse followed by a secondary component (quasiperiodic sequence of short low-intensity pulses). The oscillatory temporal structure following the main temporal component is a typical result of second-order dispersion. The Wigner distribution provides very useful information about the origin of each one of the components in the obtained temporal signal. In particular, the main temporal pulse in the resulting signal is essentially caused by the frequencies in the main spectral lobe which undergo a similar delay along the fiber (in fact, the Wigner distributions allow us to infer that this main temporal component is closely a transform-limited signal). The subsequent temporal oscillations have their origin in a spectral beating between two separated frequency bands, each one associated with each of the spectral sidelobes of the signal, which appear overlapped in time (i.e., the two beating spectral bands undergo a similar temporal delay during the fiber propagation). Note that the spectral main lobe is affected by a delay shorter than that of the spectral sidelobes (as determined by the fiber GVD). The period of the temporal oscillations is fixed by the frequency separation of the beating bands and as it can be observed, the fact that beating bands are more separated for longer delays translates into the observed oscillation period decreasing with time.

4. WIGNER ANALYSIS OF NONLINEAR PULSE PROPAGATION IN OPTICAL FIBERS

4.1. Self-phase modulation of an optical pulse

When the fiber length is such that $z \ll L_D$ but $z \approx L_{NL}$, then the pulse evolution is governed by the nonlinear effects and the GVD plays a minor role. More specifically, the nonlinear-dominant regime is applicable when the following condition is satisfied:

$$\frac{L_D}{L_{NL}} = \frac{\gamma P_0 T_0^2}{|\beta_2|} \gg 1. \tag{10}$$

In this case, the second term in the left-hand side of the NLSE in (1) (i.e., the dispersion term) can be neglected and the pulse evolution in the fiber is governed by self-phase modulation (SPM), a phenomenon that leads to spectral broadening of the optical pulse. This propagation regime will only occur for relatively high peak power when the dispersion effects can be neglected either because the fiber is operated around the zero-dispersion wavelength or because the input pulses are sufficiently wide (in a conventional single-mode fiber working at $\lambda \approx 1.55\,\mu$m, typical values for entering the SPM regime are $T_0 > 100$ picoseconds and $P_0 \approx 1\,\text{W}$).

SPM has its origin in the dependence of the nonlinear refractive-index with the optical pulse intensity (Kerr effect), which induces an intensity-dependent phase shift along the temporal pulse profile according to the following expression:

$$\begin{aligned} A(z,\tau) &= A(0,\tau)\exp\left(i\phi_{NL}(z,\tau)\right), \\ \phi_{NL}(z,\tau) &= \gamma\left|A(0,\tau)\right|^2 z. \end{aligned} \tag{11}$$

Equation (11) shows that during SPM the pulse shape remains unaffected as the SPM only induces a temporally-varying phase shift. This phase shift implies that an additional frequency chirp is induced in the optical pulse so that new frequency components are generated along the pulse profile. In particular, the SPM-induced instantaneous frequency along the pulse duration is

$$\delta\omega(z,\tau) = -\frac{\partial\phi_{NL}(z,\tau)}{\partial\tau} = -\gamma z\frac{\partial\left|A(0,\tau)\right|^2}{\partial\tau}. \tag{12}$$

Note that according to (11), the maximum SPM-induced phase-shift across the pulse is $\phi_{\text{MAX}} = \gamma P_0 z$. Figure 4 analyzes SPM of a long super-Gaussian pulse ($m = 3$ and $T_0 = 90$ picoseconds) for different values of ϕ_{MAX} (i.e., evaluated at different fiber lengths or for different pulse peak powers). The input pulse is also shown ($\phi_{\text{MAX}} = 0$). The expected spectral pulse distortion and broadening is observed in the plots. The Wigner distribution is an ideal tool to visualize the process of generation of new spectral components as it associates these new spectral components with the temporal features of the optical pulse. The Wigner distribution confirms the generation of new spectral content according to (12). In general, this spectral content generation process is more significant as ϕ_{MAX} increases. Specifically, the steeping edge of the pulse is responsible for the generation of new frequency components in the low-frequency sidelobe (negative side) whereas the trailing edge is responsible for the generation of new frequency components in the high-frequency sidelobe (positive side). The central part of the pulse, where the intensity keeps approximately constant, is only responsible for the generation of new spectral content in the narrow, central frequency band (spectral main lobe). The Wigner distribution reveals that this spectral main lobe is not a transform-limited signal but rather it exhibits a pronounced chirp which becomes more significant as ϕ_{MAX} increases. It is important to note that such important feature of the generated optical pulses cannot be inferred from the basic SPM theory presented above or through the representation of the instantaneous frequency of the signals (i.e., by calculating the derivative of the pulse phase profile).

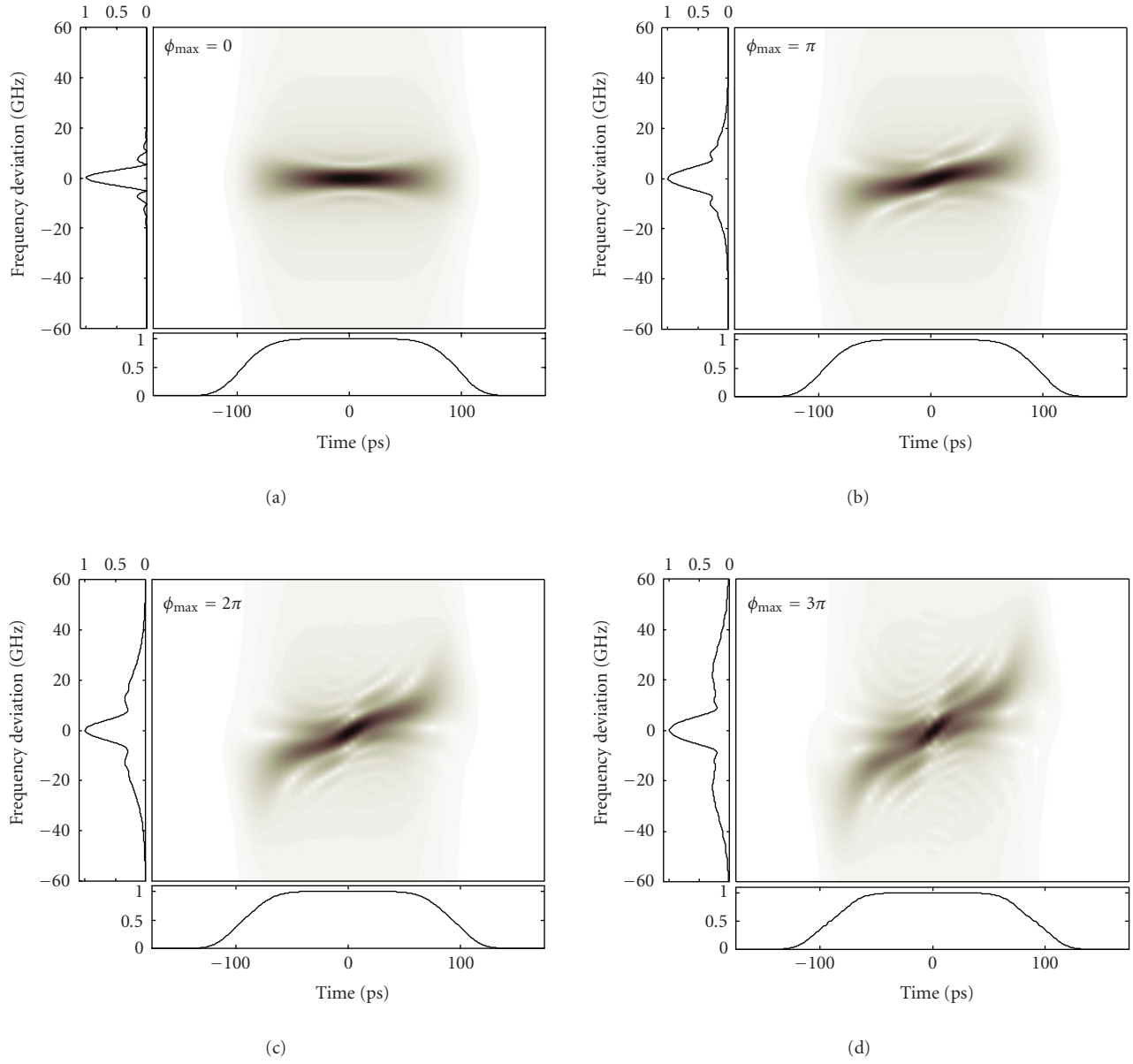

Figure 4: Wigner analysis of pulse self-phase modulation in an optical fiber.

4.2. *Dynamics of temporal soliton formation in the anomalous dispersion regime*

When the fiber length z is longer or comparable to both L_D and L_{NL}, then dispersion and nonlinearities act together as the pulse propagates along the fiber. The interplay of the GVD and SPM effects can lead to a qualitatively different behavior compared with that expected from GVD or SPM alone. In particular, in the anomalous dispersion regime ($\beta_2 < 0$) the fiber can support temporal solitons (bright solitons). Basically, if an optical pulse of temporal shape $A(0,\tau) = \sqrt{P_0}\,\mathrm{sec}\,h(\tau/T_0)$ is launched at the input of the fiber and the pulse peak power is such that it satisfies exactly the following condition $L_D = L_{NL}$, then the pulse will propagate undistorted without change in shape for arbitrarily long distances (assuming a lossless fiber). It is this feature of the fundamental solitons that makes them attractive for optical communication applications. As a generalization, if an optical pulse of arbitrary shape and a sufficiently high peak power (peak power higher than that required to satisfy the fundamental soliton condition) is launched at the input of an optical fiber in the anomalous dispersion regime, then a temporal soliton (*sech* temporal shape) will form after propagation through a sufficiently long section of fiber. The analysis of the dynamics of formation of a temporal soliton is a topic of paramount importance in understanding the nonlinear

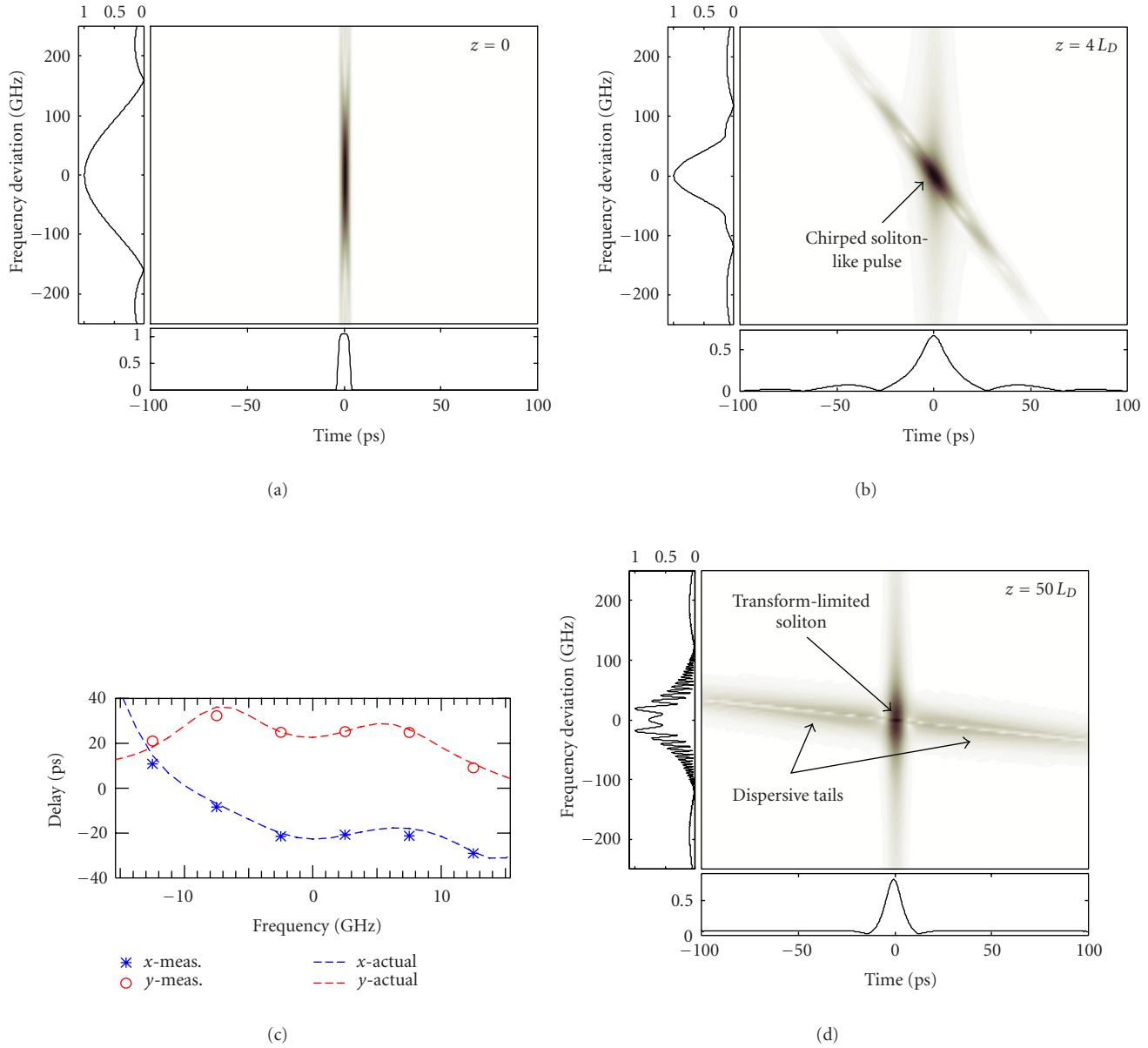

FIGURE 5: Wigner analysis of fundamental soliton formation in an optical fiber (anomalous dispersion regime).

dynamics in optical fibers and has attracted considerable attention [1, 18, 19]. Wigner analysis has been proposed as a simple and powerful method for characterizing optical soliton waveforms (e.g., to evaluate the quality of an optical soliton) [7].

Here, we analyze soliton formation dynamics when the pulse launched at the input of a fiber is not an exact soliton solution in that fiber (deviation in temporal shape). In the example of Figure 5, we assume a fiber with parameters $\beta_2 = -20\,\text{ps}^2\text{Km}^{-1}$ and $\gamma = 2\,\text{W}^{-1}\text{Km}^{-1}$ (typical values for a conventional single-mode fiber working at $\lambda \approx 1.55\,\mu$m). The input pulse is assumed to be a super-Gaussian pulse with $m = 3$, $T_0 = 3$ picoseconds and the peak power P_0 is fixed to satisfy exactly the basic first-order soliton condition, that is, $P_0 = 1.11\,\text{W}$. The Wigner representation of the optical pulse envelope $A(z, \tau)$ is evaluated at different fiber propagation distances, $z = 0$ (input pulse), $z = 4\,L_D$, $z = 20\,L_D$, and $z = 50\,L_D$. The representations in Figure 5 show that for sufficiently long distance ($z > 20\,L_D$) the original super-Gaussian pulse evolves into a signal consisting of (a) a transform-limited first-order temporal soliton and (b) two long dispersive tails. These two well-known features (soliton solution and radiation solution of the NLSE, respectively) can be visualized very clearly in the corresponding two-dimensional Wigner representations. For distances shorter than that required for soliton formation (e.g., $z = 4\,L_D$),

the characteristics patterns of the two mentioned signal components (soliton + dispersive tails) can be already distinguished in the Wigner representation but this representation shows that the main component is still a nontransform-limited (chirped) soliton-like pulse. This component is the one which finally evolves into a transform-limited soliton by virtue of the interplay between GVD and SPM. Note that when the transform-limited soliton is formed, the pulse spectrum exhibits significant oscillations. These oscillations are typical of soliton formation when the pulse launched at the input of the fiber does not satisfy the exact fundamental soliton conditions (i.e., when the input pulse is slightly different in shape, power, or chirp to the ideal soliton) [18, 19] and can be detrimental for practical applications. The fact that the input pulse must satisfy exactly the soliton conditions in order to avoid the presence of these and other detrimental effects have in part precluded the use of soliton-based techniques for communication applications. The spectral oscillations observed in our plots have been observed experimentally and a physical explanation based on complicated analytical studies has been also given [19]. The Wigner representation provides a simple and direct physical understanding of such spectral oscillations and their more significant features. In particular, these oscillations can be interpreted as Fabry-Perot-like resonance effects associated with interference between the frequencies lying in the transform-limited soliton pulse and those in the dispersive tails (i.e., same frequencies with different delays). The period of these oscillations is then fixed by the temporal delay between the interfering frequency bands. Note that the delay between interfering bands (horizontal distance in the Wigner plane) increases for a higher frequency deviation and this translates into the observed oscillation period decreasing as the frequency deviation increases. A similar explanation can be found for the observed variations in the period of the spectral oscillations as a function of the fiber length. Since the dispersive tails are affected by the fiber GVD whereas the soliton pulse is unaffected, the temporal distance between interfering bands increases as the fiber distance increases and this results into the observed oscillation period decreasing with fiber length.

4.3. Optical wave breaking phenomena in the normal dispersion regime

Soliton phenomena can also occur when the optical fiber exhibits normal dispersion ($\beta_2 > 0$) at the working wavelength. In this case, a different class of temporal solitons is possible, that is, the so-called dark soliton, which consists of an energy notch in a continuous, constant light background [1]. Although the dark soliton is of similar physical and practical interest than the bright soliton, in this section, we have preferred to focus on other similarly interesting phenomena that are typical of nonlinear light propagation in the normal dispersion regime (e.g., optical wave breaking [20, 21]) and have no counterpart in the anomalous dispersion regime.

In Figure 6, we analyze the combined action of dispersion and nonlinearities on a Gaussian pulse ($m = 1$, $T_0 = 3$ picoseconds) along a fiber with normal dispersion ($\beta_2 = +0.1\,\mathrm{ps^2Km^{-1}}$). The peak power of the pulse is fixed to ensure that the nonlinear effects (self-phase modulation, SPM) are much more significant than the dispersive effects and, in particular, $L_D = 900\,L_{NL} \approx 90\,\mathrm{Km}$, so that $P_0 \approx 5\,\mathrm{W}$. Figure 2 shows the Wigner representation of the optical pulse envelope $A(z,\tau)$ evaluated at different propagation distances, $z = 0$ (input pulse), $z = 0.02\,L_D$, and $z = 0.06\,L_D$ (note that the figure at the bottom right is a detailed analysis or "zoom" of the temporal response at $z = 0.06\,L_D$). At short distances (e.g., $z = 0.02\,L_D$), the pulse is mainly affected by SPM and as expected, the temporal variation of the spectral content (i.e., instantaneous frequency) is determined by the temporal function $\partial|A(z,\tau)|^2/\partial\tau$, see (12). The oscillations in the pulse spectrum can be interpreted again as a Fabry-Perot-like resonance effects (i.e., these oscillations have their origin in interference between the same spectral components located at different instants of time). For a distance $z = 0.06\,L_D$, the pulse energy is temporally and spectrally redistributed as a result of the interplay between dispersion and SPM [20]. The Wigner distribution provides again a simple understanding of the observed temporal and spectral pulse features. In particular, the Fabry-Perot resonance effects described above appear again and are responsible for the observed oscillations in the main spectral band. The temporal pulse evolves nearly into a square shape slightly broader than the input Gaussian pulse. This square pulse exhibits a linear frequency chirp practically along its total duration. This fact has been used extensively for pulse compression applications [17]. It is also important to note that the pulse spectrum exhibits significant sidelobes. From the Wigner representation, it can be easily inferred that these sidelobes are responsible for the observed oscillations in the leading and trailing edges of the temporal pulse. A more detailed analysis of the temporal oscillations in the trailing (leading) edge of the pulse shows that these oscillations have their origin in a spectral beating between two separated spectral bands located in the high-frequency (low-frequency) sidelobe of the pulse spectrum. The whole process by virtue of which the temporal pulse develops the described temporal oscillations in its edges associated with sidelobes in the spectral domain is usually referred to as optical wave breaking [20, 21]. Our results show that the Wigner analysis constitutes a unique approach for visualizing and understanding the physics behind this well-known phenomenon.

5. CONCLUSIONS

In summary, the Wigner analysis has been demonstrated to be a powerful tool for investigating picosecond pulse propagation dynamics in optical fibers in both the linear and nonlinear propagation regimes. This analysis provides a simple, clear, and profound insight into the nature of the physical phenomena that determine the pulse evolution in an optical fiber, in some cases revealing details about these physical phenomena which otherwise cannot be inferred.

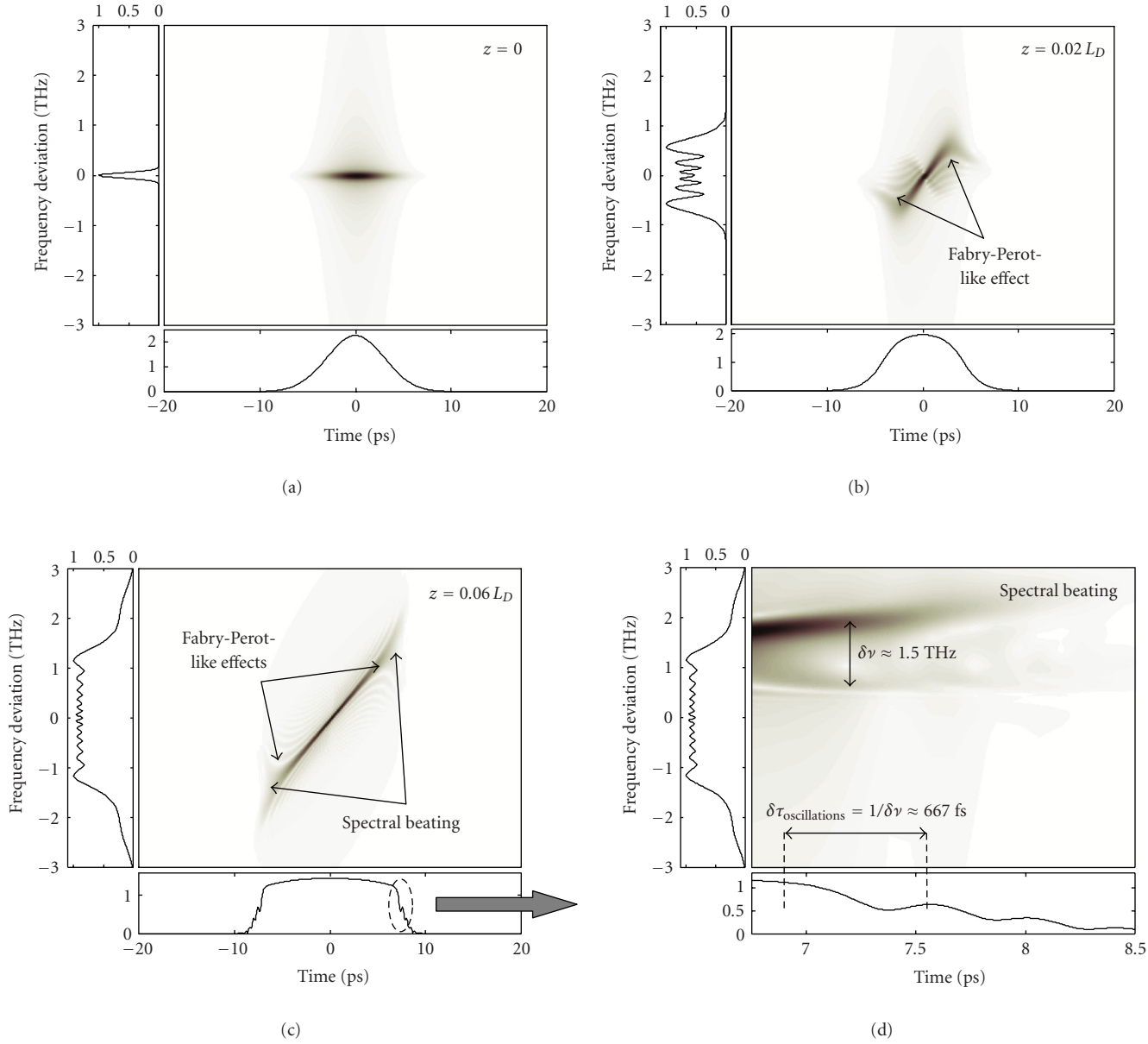

Figure 6: Wigner analysis of nonlinear pulse propagation through an optical fiber in the normal dispersion regime.

The examples in this paper demonstrate the efficiency of the TF (Wigner) techniques for the analysis of linear and nonlinear optical systems and should encourage the application of these techniques to a variety of related problems, such as the systematic study of femtosecond pulse propagation in optical fibers (i.e., influence of high-order dispersion and nonlinear effects) or spatiotemporal dynamics.

In general, the results presented here clearly illustrate how advanced signal processing tools (e.g., TF analysis) can be applied to investigating physical systems of fundamental or practical interest and how the unique information provided by these advanced analysis tools can broaden our understanding of the systems under study.

REFERENCES

[1] G. P. Agrawal, *Nonlinear Fiber Optics*, Academic Press, San Diego, Calif, USA, 3rd edition, 2001.

[2] G. P. Agrawal, *Fiber-Optic Communication Systems*, John Wiley & Sons, New York, NY, USA, 3rd edition, 2002.

[3] L. Cohen, "Time-frequency distributions—a review," *Proc. IEEE*, vol. 77, no. 7, pp. 941–981, 1989.

[4] D. Dragoman, "The Wigner distribution function in optics and optoelectronics," *Progress in Optics*, vol. 37, pp. 1–56, 1997.

[5] J. Paye, "The chronocyclic representation of ultrashort light pulses," *IEEE J. Quantum Electron.*, vol. 28, no. 10, pp. 2262–2273, 1992.

[6] J. Azaña and M. A. Muriel, "Study of optical pulses—fiber gratings interaction by means of joint time-frequency signal representations," *IEEE/OSA J. Lightwave Technol.*, vol. 21, no. 11, pp. 2931–2941, 2003.
[7] D. Dragoman and M. Dragoman, "Phase space characterization of solitons with the Wigner transform," *Optics Communications*, vol. 137, no. 4–6, pp. 437–444, 1997.
[8] V. J. Pinto-Robledo and T. A. Hall, "Chronocyclic description of laser pulse compression," *Optics Communications*, vol. 125, no. 4–6, pp. 338–348, 1996.
[9] K. Mochizuki, M. Fujise, M. Kuwazuru, M. Nunokawa, and Y. Iwamoto, "Optical fiber dispersion measurement technique using a streak camera," *IEEE/OSA J. Lightwave Technol.*, vol. 5, no. 1, pp. 119–124, 1987.
[10] N. Nishizawa and T. Goto, "Experimental analysis of ultrashort pulse propagation in optical fibers around zero-dispersion region using cross-correlation frequency resolved optical gating," *Optics Express*, vol. 8, no. 6, pp. 328–334, 2001.
[11] J. M. Dudley, X. Gu, L. Xu, et al., et al., "Cross-correlation frequency resolved optical gating analysis of broadband continuum generation in photonic crystal fiber: simulations and experiments," *Optics Express*, vol. 10, no. 21, pp. 1215–1221, 2002.
[12] L. Helczynski, D. Anderson, R. Fedele, B. Hall, and M. Lisak, "Propagation of partially incoherent light in nonlinear media via the Wigner transform method," *IEEE J. Select. Topics Quantum Electron.*, vol. 8, no. 3, pp. 408–412, 2002.
[13] D. Yevick and B. Hermansson, "Soliton analysis with the propagation beam method," *Optics Communications*, vol. 47, no. 2, pp. 101–106, 1983.
[14] Y. C. Tong, L. Y. Chan, and H. K. Tsang, "Fibre dispersion or pulse spectrum measurement using a sampling oscilloscope," *Electronics Letters*, vol. 33, no. 11, pp. 983–985, 1997.
[15] J. Azaña and M. A. Muriel, "Real-time optical spectrum analysis based on the time-space duality in chirped fiber gratings," *IEEE J. Quantum Electron.*, vol. 36, no. 5, pp. 517–526, 2000.
[16] P. C. Chou, H. A. Haus, and J. F. Brennan III, "Reconfigurable time-domain spectral shaping of an optical pulse stretched by a fiber Bragg grating," *Optics Letters*, vol. 25, no. 8, pp. 524–526, 2000.
[17] W. J. Tomlinson, R. H. Stolen, and C. V. Shank, "Compression of optical pulses chirped by self-phase modulation in fibers," *Journal of the Optical Society of America B*, vol. 1, no. 2, pp. 139–149, 1984.
[18] C. Desem and P. L. Chu, "Effect of chirping on solution propagation in single-mode optical fibers," *Optics Letters*, vol. 11, no. 4, pp. 248–250, 1986.
[19] M. W. Chbat, P. R. Prucnal, M. N. Islam, C. E. Soccolich, and J. P. Gordon, "Long-range interference effects of soliton reshaping in optical fibers," *Journal of the Optical Society of America B*, vol. 10, no. 8, pp. 1386–1395, 1993.
[20] W. J. Tomlinson, R. H. Stolen, and A. M. Johnson, "Optical wave breaking of pulses in nonlinear optical fibers," *Optics Letters*, vol. 10, no. 9, pp. 457–459, 1985.
[21] J.-P. Hamaide and Ph. Emplit, "Direct observation of optical wave breaking of picosecond pulses in nonlinear single-mode optical fibres," *Electronics Letters*, vol. 24, no. 13, pp. 818–819, 1988.

José Azaña was born on December 8, 1972, in Toledo, Spain. He received the Ingeniero de Telecomunicación degree (a six-year engineering program) and the Ph.D. degree (in the areas of optical signal processing and fiber Bragg gratings) from the Universidad Politécnica de Madrid (UPM) in 1997 and 2001, respectively. From September 2001 to mid 2003, he worked as a Postdoctoral Research Associate in the Department of Electrical and Computer Engineering, McGill University, and he was recently appointed by the Institut National de la Recherche Scientifique, Montreal, as an Assistant Research Professor. His current research interests focus on fiber and integrated technologies for ultrafast optical signal processing and for optical pulse shaping.